

## Recent Advances in Analytical Satellite Theory

E. M. Gaposchkin  
 Smithsonian Astrophysical Observatory  
 Cambridge, Massachusetts 02138

**Abstract.** Recent work on analytical satellite-perturbation theory has involved the completion of a revision to 4th order for zonal harmonics, the addition of a treatment for ocean tides, an extension of the treatment for the noninertial reference system, and the completion of a theory for direct solar-radiation pressure and earth-albedo pressure. Combined with a theory for tesseral-harmonics, lunisolar, and body-tide perturbations, these formulations provide a comprehensive orbit-computation program. Detailed comparisons with numerical integration and observations are presented to assess the accuracy of each theoretical development.

## Introduction

Attempts to find analytical descriptions of satellite motion predate the age of artificial earth satellites. The considerable body of theory in existence at that time became the foundation on which to build solutions to specific problems arising from the desire to calculate trajectories of artificial satellites. The celebrated volume 64 of the *Astronomical Journal* can be considered the beginning of the field of celestial mechanics for satellite geodesy. Three papers in particular appeared in that issue [Brouwer, 1959; Garfinkel, 1959; Kozai, 1959]; of these authors, Garfinkel and Kozai are contributing to the field today. Those articles all address essentially the same problem — perturbations due to  $J_2$ ,  $J_3$ , and  $J_4$  — and are significant in two respects: That problem is still receiving attention, and the methods employed then are still in use. One part of this paper is devoted to what is called the main problem of satellite theory; some of the present results will be reviewed. The method used then by Kozai to integrate the Lagrange planetary equations is almost commonplace now. The device of canonical transformations employed by Brouwer and Garfinkel is now used almost exclusively when higher order solutions are developed for specific problems. The von Ziepel method of finding a canonical transformation led to a significant generalization by Horri [1966, 1973] in the method of Lie Series, a method that has become the *sine qua non* of modern methods. Just because the beginning work was similar to the present, however, does not mean that no progress has been made. On the contrary, enormous strides have been taken and considerable work probably remains.

The main motivation for developing elaborate analytical descriptions for satellite motion is to aid in understanding the forces causing the motion. A second practical reason is the potential economy available for certain applications. As our understanding of the driving forces increases and as the observational accuracy improves, the requirements for accuracy become correspondingly stringent. An accuracy goal — say 1 cm — is easily

set, but how to verify that an accuracy has been achieved is not so clear.

In 1967, I presented a paper similar to this one [Gaposchkin, 1968], describing a philosophy of how to develop, combine, and verify a complete satellite theory and outlining the status at that time. Basically, the method consisted of two steps — a comparison with numerical integration to verify that the mathematical problem had been properly solved, followed by a comparison with observations to verify that the mathematical problem was an adequate description of the physical problem. I am not so optimistic now. First, preserving the accuracy of numerical-integration methods for long time periods poses considerable problems [Velez, 1975; Balmino, 1975]. In this context, a long period is measured in terms of the number of revolutions of the fastest body, normally the satellite; integrations for more than 1000 revolutions of anything are difficult and time consuming. Although the theory can be used to test the integration, rather than the other way around, even the use of numerical integration to test short-period perturbations has proved difficult. Second, verifying the theory by means of data analysis presents significant problems. Many cases occur in which several forces have similar qualitative orbital effects that tend to cancel. A good example is shown by lunar and solar perturbations, where the direct effects, the effects due to tidal deformation, and the effects due to precession and nutation all have the same origin and produce perturbations with the same spectral character; in some cases, these effects add, and in others, they cancel. A third aspect of this verification process is the necessity to know certain physical quantities. While this is not a problem in the comparison with numerical integration, it is critical in the analysis of observations. In reality, then, the verification must be combined with the determination of physical quantities. Finally, although individual components of the satellite theory can be verified, in practical terms, the theory must all fit together and several interactions should be taken into account. Indeed, there are significant difficulties, but the situation is far from hopeless, and in the following, I describe where we are today in the theory, the verification, and the data analysis.

## Selection of Variables

The first thing to select is a set of variables to be used for the analysis. The most popular set is the Kepler elements ( $\omega$  = argument of perigee,  $\Omega$  = right ascension of the ascending node,  $I$  = inclination,  $e$  = eccentricity,  $M$  = mean anomaly, and  $a$  = semimajor axis). In practice,  $a$  is obtained from the mean motion  $n$  according to Kepler's third law  $n^2 a^3 = \text{constant}$ , and  $n$  then becomes the sixth variable. This is done for the practical reason that  $n$  is the more easily and more accurately determined quantity, and  $a$  becomes a derived quantity. This set of variables has the conceptual

advantage that each has a simple physical meaning. Kepler elements have the one drawback that for zero eccentricity or inclination, they become degenerate. This degeneracy is also a problem for small eccentricities and inclinations, in that these variables become highly correlated in any adjustment procedure that attempts to determine them by a statistical process using observations. Finally, this degeneracy presents analytical difficulties; some series expansions become much longer than they would if another set of variables were chosen. Nevertheless, Kepler elements continue to be the most widely used both for analytical work and for reporting results.

For the reason cited above, some fundamental analysis is now done with another set of variables; a list of candidate variables was given by Gaposchkin [1973]. For the following, the inclination degeneracy has not been addressed, but the more important and relevant degeneracy in eccentricity has been overcome by using the nonsingular variables

$$\xi = e \cos \omega, \quad \eta = e \sin \omega, \quad M + \omega, \quad \Omega, \\ L^2 = a, \quad H = G \cos I,$$

where

$$G^2 = L^2(1 - e^2) = L^2(1 - \xi^2 - \eta^2).$$

In that set of variables,\* the Kepler elements are recognizable, along with the Delaunay variables  $l = M$ ,  $g = \omega$ ,  $h = \Omega$ ,  $L$ ,  $G$ , and  $H$ . The Delaunay variables are used to derive the long-period and secular perturbations and are then formally combined into the set of nonsingular variables for numerical evaluation. It can be shown that these nonsingular variables satisfy the d'Alembert characteristic with respect to eccentricity, although not with respect to  $\sin I$ . The d'Alembert characteristic is that the lowest powers of  $e$  and  $\sin I$  of the coefficient  $\frac{\sin}{\cos}(kM + q\omega)$  in the trigonometric series are  $\alpha$  and  $\beta$ , respectively, where

$$\alpha = |k - q| \pmod{2}, \\ \beta = |q| \pmod{2}.$$

Therefore, any expression satisfying the d'Alembert characteristic is well behaved as  $e$  (or  $\sin I$ ) goes to zero. If it is necessary to compute perturbations for small inclinations, then the variable  $M + \omega + \Omega$  satisfies the d'Alembert characteristic and is suitable.

For the main problem, we have formally obtained expressions for the nonsingular variables analytically. However, if the computer word has sufficient accuracy, then the nonsingular variables can be calculated numerically, and the well-conditioned properties of these variables can be realized. Therefore, it is entirely adequate, if necessary, to derive perturbations in Kepler elements and numerically combine them into non-

\* Expressions are often written in this expanded set of variables, but formally, this is only a notational convenience.

singular variables for calculating an ephemeris. Of course, a unified treatment in nonsingular variables would be preferable, although it is not always the most convenient solution. We can then develop perturbations in the most convenient set of variables for the particular problem and then unify the variables at the calculation stage.

Mean elements are a key to the construction of an analytical theory. In the framework of perturbation theory, the mean elements are the zero-order reference for the development. They become the constants of integration and therefore play a similar role to the initial conditions in solving differential equations. Each perturbation theory has implicit in it a definition of mean elements, and generally the relation between mean elements and the initial conditions does not receive any attention.

In the present situation, several perturbation theories are employed in the same computation, with the mean elements being empirically obtained from observations. This situation is rigorously correct when a single perturbation theory is employed, provided suitable partial derivatives are available. In the general case, the mean elements must have the same formal definition, to the accuracy of the theory.

A second aspect of mean elements concerns their constancy. If they were truly constants of the motion, if we knew all the numerical constants entering the theory, and if our observations were without error, then the mean elements for a satellite would be the same at different epochs. Any variations in them would have to be due to errors in the theory, errors in some numerical constants, or errors in the data. Assuming that we can control errors in the theory and the data, then the variations in the mean elements can be used to get information on the numerical constants (i.e., the physical parameters) entering the orbit theory. In fact, this has been the basis of much of the geodetic and geophysical information obtained from satellite data.

#### Analytical Methods

Basically, three methods are used to develop satellite theory. To begin with, we cannot hope to find exact closed-form solutions to the equations of motion and must seek approximate solutions by some perturbation method. The simplest method is to recast the equations of motion in our chosen set of variables, for example, Kepler elements. This results in a rigorously equivalent set of six coupled first-order differential equations, called the Lagrange planetary equations. For some perturbations (for example, for tesseral harmonics), we can expand these variables around a reference orbit, say a precessing Keplerian ellipse, by Fourier series. The equations can then be treated as a forced harmonic oscillator with constant coefficients, and this approximation to the equations of motion can be integrated term by term. The approximation can be further improved by using this first-order solution as the reference orbit, expanding it in Fourier series, and so on. Beyond the second order, however, the method is usually replaced by the more general one of canonical transformation.

The theory of canonical transformation goes back to the last century, when it was developed to solve mechanics problems. It uses more fundamental properties of dynamical systems, which are beyond the scope of this discussion. Suffice it to say that it is rigorously equivalent and can be either easier or more difficult than the use of Lagrange planetary equations. Originally, canonical-transformation theory was thought to require the use of canonical variables, but the generalization by Hori [1966] proved that it can be employed for any variable provided the basic equations can be solved. In the theory of canonical transformation, the key is to find a solution to a single partial-differential equation. Although in general this is difficult, a method has been developed for the satellite main problem that will automatically find a suitable approximation to the equation. Therefore, this method is applicable to obtaining a solution to any order and can be automated, to some extent, on a computer. Such an approach is in general use now for higher order solutions.

When the first two methods are inadequate for some reason, a third one must be used. This is called a semianalytical solution, in that part of the solution (integration) can be accomplished analytically, while the remaining part must necessarily be done numerically. Recourse to this method is required when closed-form expressions for the force function are complicated or impossible to find. Examples are lunisolar perturbations when the analytical description of the moon's motion to suitable accuracy would be prohibitive and radiation-pressure perturbations when the shadow function must be obtained numerically. This method integrates over the short-period perturbation analytically and then integrates the averaged force function numerically to obtain the perturbations. In this case, the numerical integration can take relatively large time steps and is therefore economical. It also conveniently separates long-period and short-period perturbations.

#### Current Status

A third-order solution to the main problem — i.e., for the motion of a satellite in the geopotential containing only  $J_2$ ,  $J_3$ , and  $J_4$  — has been obtained by Kinoshita [1977]. Third-order periodic perturbations with fourth-order secular perturbations are derived by the method due to Hori [1966]. All quantities are expanded into power series in the eccentricity, but the solution is closed with respect to inclination. A comparison with results obtained by numerical integration of the equations of motion indicates that the solution can predict the position of a close-earth satellite with an accuracy of better than 1 cm over a period of 1 month. For this check, a special-purpose Taylor-type integrator is adopted, in which the positions and velocities are expanded into a power series of time and the coefficients of the series are determined by recurrence formulas [Rabe, 1961; Deprit and Zahar, 1966].

Periodic perturbations due to tesseral harmonics are a first-order linear theory based on integration of the Lagrange planetary equations as

developed by Kaula [1966]. The theory also includes the interaction with  $J_2$  and second-order interactions with the mean motion through Kepler's third law. Although the theory is essentially that of Kaula, the details of the calculation have been considerably revised with the inclination function as described by Gaposchkin [1973] or Kinoshita [1977] and the eccentricity function calculated as Hansen coefficients.

The lunisolar perturbations in satellite motion are obtained by a semianalytical method [Kozai, 1973]. The disturbing function is expressed by the orbital elements of the satellite and the geocentric polar coordinates of the moon and the sun. These coordinates are obtained by using the larger terms in Brown's theory [United States Naval Observatory, 1954]: 26 terms in longitude, 14 in latitude, and 12 in the parallax. The secular and long-period perturbations are derived by numerical integration, and the short-period perturbations, analytically. Perturbations due to the solid body tide can be included in the same way.

The orbital elements of a close-earth satellite have perturbations caused by the motion of the equatorial plane of the earth due to precession and nutation. Kozai and Kinoshita [1973] derived exact differential equations for the perturbations of satellite orbital elements due to the motion of the earth's equatorial plane and solved them to second order in precession. This theory, in fact, defines the reference system used for satellite motion, in which the inclination and the argument of perigee are referred to the equator of date and the longitude of the ascending node is measured from a fixed point along a fixed plane and then along the equator of date.

The perturbations of a spherical satellite due to direct solar radiation are computed according to a semianalytical algorithm due to Aksnes [1976], which is based on expressions derived by Kozai [1961]. Through some simple modifications, the algorithm also holds when  $e = 0$  and  $i = 0$ . The perturbations are obtained by summing over the sunlit segment of the satellite's orbit during each revolution or partial revolution. The end points of the segment are evaluated numerically once per revolution. Testing of the algorithm is done by means of numerical integration of the equations of motion and through comparisons with observations of the balloon satellite 1963 30D during a 200-day interval.

The perturbations due to solar radiation diffusely reflected from the earth have been treated by Lautman [1977a], who used a semianalytical method based on the assumptions that the satellite is spherically symmetric and that solar radiation is reflected from the earth according to Lambert's law with uniform albedo. Expressions for the radiation-pressure force are developed into series in true anomaly  $v$ . The perturbations within a given revolution are obtained analytically by integrating with respect to  $v$ , while holding all slowly varying quantities constant. The long-term perturbations are then obtained by summing the net perturbations at the end of each revolution. This theory has been extended [Lautman, 1977b] to account for the increasing reflectivity of the earth toward the poles; the earth's albedo is assumed to have a latitude dependence given by  $a = a_0 + a_2 \sin^2 \phi$ .

The short-period perturbations due to air drag are computed according to a computation due to Sehna and Mills [1966]. The density function of the earth's atmosphere includes the effect of the atmospheric bulge described by Jacchia. The method of solution is, in essence, numerical construction of the disturbing function. The secular acceleration for geodetic satellites is more accurately given by analysis of the data. The short-period perturbation is usually less than 1 cm per revolution, and this development is not currently used.

The analysis of ocean tides is done along the following lines. Recall that in calculating luni-solar perturbations, the body-tide potential is easily included by introducing the Love number  $k_\ell$ . An alternative way to describe the lunisolar gravitational potential is essentially given by Doodson [1921]. In this case, the potential at the earth's surface can be written

$$\frac{U}{g} = \text{Re} \sum_{\ell m s} F_{\ell m} D_{\ell m s} (i)^{\ell+m} (-1)^{[(\ell+m+1)/2]} \times \bar{P}_{\ell m}(\phi) e^{i(\sigma_s(t)+m\lambda)}$$

where  $\text{Re}\{x\}$  is the real part of  $x$ ,  $i^2 = -1$ ,  $[x]$  is the integer part of  $x$ ,  $F_{\ell m}$  are numerical factors,  $D_{\ell m s}$  are the  $s$  coefficients as determined by Doodson by Fourier analysis,  $\bar{P}_{\ell m}$  are fully normalized associated Legendre functions, and  $\sigma_s(t)$  is the time variation given in terms of the six chosen variables.

Cartwright and Edden [1973] have provided values of  $D_{\ell m s}$  based on modern values of the solar and lunar ephemerides:  $F_{20} = -12.020364$  cm,  $F_{21} = F_{12} = 13.879920$  cm. Expression (1) is the potential at the surface of the earth, and we can continue this potential analytically to satellite altitudes as

$$\frac{U}{g} = \text{Re} \sum_{\ell m s} \left(\frac{r}{a_e}\right)^\ell F_{\ell m} D_{\ell m s} (i)^{\ell+m} (-1)^{[(\ell+m+1)/2]} \times \bar{P}_{\ell m}(\phi) e^{i(\sigma_s(t)+m\lambda)}$$

and then develop satellite perturbations due to the sun and the moon. The body tide can be defined in terms of the complex Love number

$$k_\ell^* = k_\ell \left(1 - i \frac{\mu}{2Q}\right)$$

[Munk and MacDonald, 1960, p. 153]. Considering the deformation,  $U_{\text{tide}}$  can be analytically continued to satellite altitudes as

$$U_{\text{tide}} = g \text{Re} \sum_{\ell m s} \left(\frac{a_e}{r}\right)^{\ell+1} k_\ell^* F_{\ell m} D_{\ell m s} \times (i)^{\ell+m} (-1)^{[(\ell+m+1)/2]} \bar{P}_{\ell m}(\phi) \times e^{i(\sigma_s(t)+m\lambda)}$$

Similarly, each component of an ocean tide of height  $\zeta_s$  (for driving function  $D_{\ell m s}$  for argument  $\sigma_s$ ) can be expressed in spherical harmonics  $\mathcal{C}_{\ell m s}$ ,

where  $\mathcal{C}_{\ell m s}$  is the fully normalized complex representation of the ocean tide. If the ocean tide is expressed as a surface layer, then the external potential at satellite heights can be written

$$U_{\text{ocean}} = 4\pi G \rho_\omega a_e \text{Re} \sum_{\ell m s} \frac{1 + k'_\ell}{2\ell + 1} \left(\frac{a_e}{r}\right)^{\ell+1} \times (i)^{\ell+m} (-1)^{[(\ell+m+1)/2]} \mathcal{C}_{\ell m s} \times \bar{P}_{\ell m}(\phi) e^{i(\sigma_s(t)+m\lambda)} \quad (1)$$

As noted by many [Gaposchkin, 1973; Lambeck et al., 1974; Felsentreger et al., 1976; Goad and Douglas, 1978], the ocean and body tides enter the potential in exactly the same form, and by satellite analysis, we can sense only the linear combinations,

$$g F_{\ell m} D_{\ell m s} k_\ell^*(s) + 4\pi G \rho_\omega a_e \frac{1 + k'_\ell(s)}{2\ell + 1} \mathcal{C}_{\ell m s}$$

where  $k_\ell$  and  $k'_\ell$  are assumed to depend on the frequency of the argument  $\sigma_s$ . Thus, we are obliged to assume one tide to determine the other.

For frequencies far from resonance ( $23^{\text{h}}53^{\text{m}}05^{\text{s}}04$ ),  $k_\ell$  and presumably  $k'_\ell$  can be taken from seismic models [Longman, 1962, 1963; Farrell, 1972]. Both Jeffreys and Vicente [1957a,b] and Molodensky [1961] pointed out that nearly diurnal earth tides should be amplified because of the existence of a resonance between the elastic mantle and the liquid core. In Table 1, the variation in  $k_2$  predicted by Molodensky's Model II is given.

In any event, the expressions for the potentials [eqs. (2) through (4)] can easily be used to obtain satellite perturbations, as the arguments are given as linear functions of time, and the Lagrange planetary equations can be integrated directly as a forced harmonic oscillator.

#### Accuracy Assessment

The various perturbation theories described above are all included in a general-purpose orbit-determination program that accepts observations of direction, range difference, and range rate. Each individual theory has been tested, and now we wish to study the accuracy of the combined theory. For this purpose, we used a numerical integration program to calculate simulated (errorless) data. The general-purpose integration program, developed by Krogh [1973], is an Adams-type integrator that has the option of variable or fixed step size once the integration has been started. The variable-step-size option uses a desired accuracy as input. The program performs the integration in coordinates  $(x, y, z, \dot{x}, \dot{y}, \dot{z})$  in single precision on a CDC 6000 computer that has 14-decimal-digit accuracy. The force package allows use of an arbitrary gravity field represented in spherical harmonics, moon and sun positions (we use the same routines as the analytical theory), radiation pressure, and a drag model based on the same physical assumptions as the analytical developments described earlier.

TABLE 1. Values of  $k_2$  for Tidal Terms Near Resonance  
(Based on Molodensky, 1961)

| Doodson | Darwin          | $D_{\text{rms}}$ | $\beta$ | $k_2$  | $\sigma$ ( $^\circ/\text{hr}$ ) |
|---------|-----------------|------------------|---------|--------|---------------------------------|
| 255.555 | M2              | 0.90809          | 0.84    | 0.3015 | 28.984104                       |
| 185.555 | 00 <sub>1</sub> | -0.01624         | -4.54   | 0.3025 | 16.139102                       |
| 167.555 | $\phi_1$        | -0.00755         | -124.06 | 0.3277 | 15.123206                       |
| 166.554 | $\psi_1$        | -0.00422         | -728.10 | 0.4551 | 15.082135                       |
| 165.565 |                 | -0.07186         | 206.19  | 0.2580 | 15.043275                       |
| 165.555 | K1              | -0.53011         | 192.30  | 0.2609 | 15.041069                       |
| 165.545 |                 | 0.01051          | 180.17  | 0.2635 | 15.038862                       |
| 163.555 | P1              | 0.17543          | 55.49   | 0.2898 | 14.958931                       |
| 145.555 | O1              | 0.37694          | 6.79    | 0.3001 | 13.943036                       |
| 056.554 | SA              | 0.01156          | 1.70    | 0.3015 | 0.041067                        |

$$\beta = \frac{41.87}{0.2136 - 100[(\sigma + w)/\sigma]} + 1.9$$

$$k_2 = 0.3015 + 0.2109 \times 10^{-3} \frac{\sigma(\sigma + 2w)}{w^2} \beta$$

where  $\sigma = \theta - w$ ,  $\sigma$  being the external driving frequency and  $\theta$  being the earth-fixed driving frequency.

We originally planned to use simulated data to verify the short-period perturbations, largely because we believed that the accuracy of a general-purpose numerical integration could not be relied on, but secondarily to conserve computer time. For the short-period perturbations, simulated range observations were computed for subsets of the forces. The simulated observations were used in the general orbit-determination program, and the mean elements were computed by least squares, thus avoiding the problem of explicitly relating the initial conditions of the numerical integration and the mean elements. This testing was done for satellites in orbits similar to those of Geos 1 and Geos 3. Our main interest was the difference in eccentricity between the two satellites, as one of our concerns was the validity of solutions for small eccentricity. The results of this testing are given in Table 2.

During the first phase of the study, the variable step size was exercised in the numerical integration; the accuracy sought was  $10^{-4}$  cm/sec. Because of the excellent agreement of the theory for the main problem ( $J_2, J_3, J_4$ ), the integration ephemeris was thought to be of sufficient accuracy. However, when working with a combined tesseral- and zonal-harmonics field, the accuracy never was better than 19 cm root mean square. The tesseral-harmonics theory alone (with  $J_2 = 0$ ) gave perfect agreement.

Since their amplitudes are approximately 1 m, the  $J_2$  interaction terms could be suspect, but they have been carefully checked by me and by H. Kinoshita. Furthermore, if the interaction terms need revision, we would expect that adding more harmonics would increase the error. In fact, increasing the field from  $C_{22}, S_{22}$  to the complete field through  $C_{44}, S_{44}$  (i.e., eight times the number of coefficients) only decreased the goodness of fit, from 19 to 22 cm.

At that point, the accuracy of the integrator

was questioned, and some simple tests were made with fixed-step-size runs. In all cases, the trajectories differed by more than 1 m. For example, the difference between the variable step size and the fixed 0.25-sec step size can be written rather well as

TABLE 2. Test of Orbit Determination

| Force Function                                      | Interval (days) | Geos 1 $\sigma$ (m) | Geos 3 $\sigma$ (m) |
|---|-----------------|---------------------|---------------------|
| $J_2$   | 1               | 0.01                | 0.01                |
| $J_2, J_3, J_4$                                     | 1               | 0.01                | 0.01                |
| $J_2, J_3, J_4, J_5$                                | 1               | 0.04                |                     |
| $J_2, J_3, J_4$                                     | 12              |                     | 0.06                |
| $J_2, C_{22}, S_{22}$                               | 1               | 0.19                |                     |
| $C_{22}, S_{22}$                                    | 1               | 0.01                |                     |
| $J_2, J_3, J_4, C_{22} - S_{44}$                    | 1               | 0.22*               |                     |
| $J_2, J_3, J_4, C_{22} - S_{44}$                    | 6               | 0.36                |                     |
| $J_2 + \text{sun} + \text{moon} + \text{body tide}$ | 1 <sup>†</sup>  | 0.12                |                     |
| Sun + moon + body tide                              | 1 <sup>†</sup>  | 0.12                |                     |
| $J_2 - S_{44}$                                      | 1               | 0.25 <sup>‡</sup>   |                     |
| $J_2 - S_{44}$                                      | 1               | 0.24**              |                     |

\* The integrator used a variable step size.

† The dynamical effects of the moving equator are not included in either the numerical integrator or the analytical theory.

‡ The integrator used a fixed step size of 0.5 sec.

\*\* The integrator used a fixed step size of 0.25 sec.

$$\epsilon = 250 t^3 \text{ cm}$$

where  $t$  is in days. Two trajectories that differ by more than 2.5 m can be fit to an accuracy of 22 cm. Clearly, the process of fitting mean elements was able to adjust or compensate for the difference between the two trajectories. This difference is due to errors in the numerical-integration algorithm, and at this point, it is not known what is the true trajectory. The nature of the integration error is that much of it can be absorbed in the mean elements of the analytical theory. In fact, this should not be surprising. An along-track acceleration can be modeled by a change in the mean motion. In any event, what can be said is that short-period perturbations can be modeled with an accuracy of 22 cm. The limiting factor in this assessment may be either the theoretical expressions or the trajectory; further investigation is warranted.

A similar situation obtains in the case of lunisolar perturbations, where the principal effects are of much longer period than 1 day and cannot be evaluated with such a short interval. The short-period terms have an amplitude of about 1 m for Geos-type satellites. From the tests outlined in Table 2, these terms are computed to 12 cm, or about 10%. We could expect to have more than two digits even from the simplest theory. The lunisolar perturbations and the tesseral harmonics share the common factor that the disturbing function explicitly contains the time. This is not true for the zonal harmonics, where the disturbing function depends only on position. This factor may limit the accuracy of either the numerical integration or the analytical solutions.

#### Analysis of the Data

Analysis of tracking data is performed primarily to obtain geophysical information; a secondary consideration is verification of the models. (In the latter, I do not include the determination of numerical parameters, which fall under the primary objective.) In the results given here, both considerations are important. The first set of data will concern the Lageos satellite, which has exhibited some small and unexpected orbital changes. The second set of data is on the Geos 1 and Geos 2 satellites, which provide useful information about ocean tides and core-mantle resonance. Since in both cases the results cannot be unambiguously checked, they are open to interpretation and are potentially subject to errors or oversights in the very complex software packages used in analyzing tracking data.

The Lageos satellite was designed to be a stable platform, with a well-defined orbit. Its orbital characteristics, given in Table 3, were carefully chosen in several respects: The orbit is sufficiently high that the effects of the anomalous gravity field are reduced, minimizing the uncertainty in ephemeris calculation. The mean motion minimizes any resonances with the gravity field. The very small area-to-mass ratio reduces the size of nongravitational perturbations (solar pressure, albedo pressure, and atmospheric drag). The symmetrical cross section allows

TABLE 3. Orbital Characteristics of Lageos

|       |                                  |
|-------|----------------------------------|
| $a$   | $= 12.270 \times 10^6 \text{ m}$ |
| $e$   | $= 0.0046$                       |
| $I$   | $= 109^\circ 86$                 |
| $n$   | $= 6.3866 \text{ rev/day}$       |
| $A/m$ | $= 0.0069 \text{ cm}^2/\text{g}$ |

greatest ease in attempting to model these forces. Most important is that Lageos is equipped with cube-corner reflectors, which enables precision laser ranging to be done. Orbits for the first 586 days of the satellite's lifetime have been computed, from which it can be immediately seen that indeed the overall objectives have been met and the orbit is known very well.

Figure 1 is a plot of the semimajor axis of Lageos. These are independently determined values, each based on 8 days of tracking data. The perturbations described above have all been included, and the remarkable 50-cm decrease in the semimajor axis is an unmodeled effect. A candidate source for this effect is the use of an inappropriate value of  $A/m$  in calculating radiation-pressure and albedo perturbations. Over this interval, the radiation pressure contributed a 20-cm decrease in the semimajor axis, and the albedo, an additional 10 cm. To compensate for the full 50-cm decrease, however,  $A/m$  would have to be increased by a factor of 2.7, far outside the plausible uncertainty in  $A/m$ ; in addition, increases in the specular diffuse coefficient, which ranges from 1 to 1.44, and in the solar constant would be necessary. A second candidate is drag from the neutral atmosphere. The equivalent drag is enormous, amounting to that occurring at altitudes of 2000 km, but adding significant drag will reduce the good agreement in other orbital elements. In fact, most atmospheric models do not attempt to model drag above 2000 km, and our knowledge of atmospheric drag at 6000-km altitudes is extremely limited. Some sort of charge buildup and interaction with the magnetosphere is also possible, and a model of that should be explored. However, we would expect to see some change in  $\dot{a}$  corresponding to changing magnetospheric conditions. Nonisotropic radiation of heat is another possibility. Again, we would expect to see a change as the spacecraft spins down. A final possibility is the Poynting Robertson effect [Robertson, 1937]. This effect, which is viewed in celestial mechanics as an aberration, is due to the conservation of momentum of photons reradiated from the satellite both along and opposite the motion. The effect is always along track and has the same effect as drag; it can be calculated based on the incoming flux or in terms of the temperature at which the photons are reradiated. This distinction is important if radiation from the earth contributes significantly to the temperature of the satellite.

Figure 2 presents the variation in inclination for Lageos over the same period. Owing to the essentially equatorial distribution of laser tracking stations, the satellite is not observed at maximum latitude and the inclination is not so well determined as possible. With improved

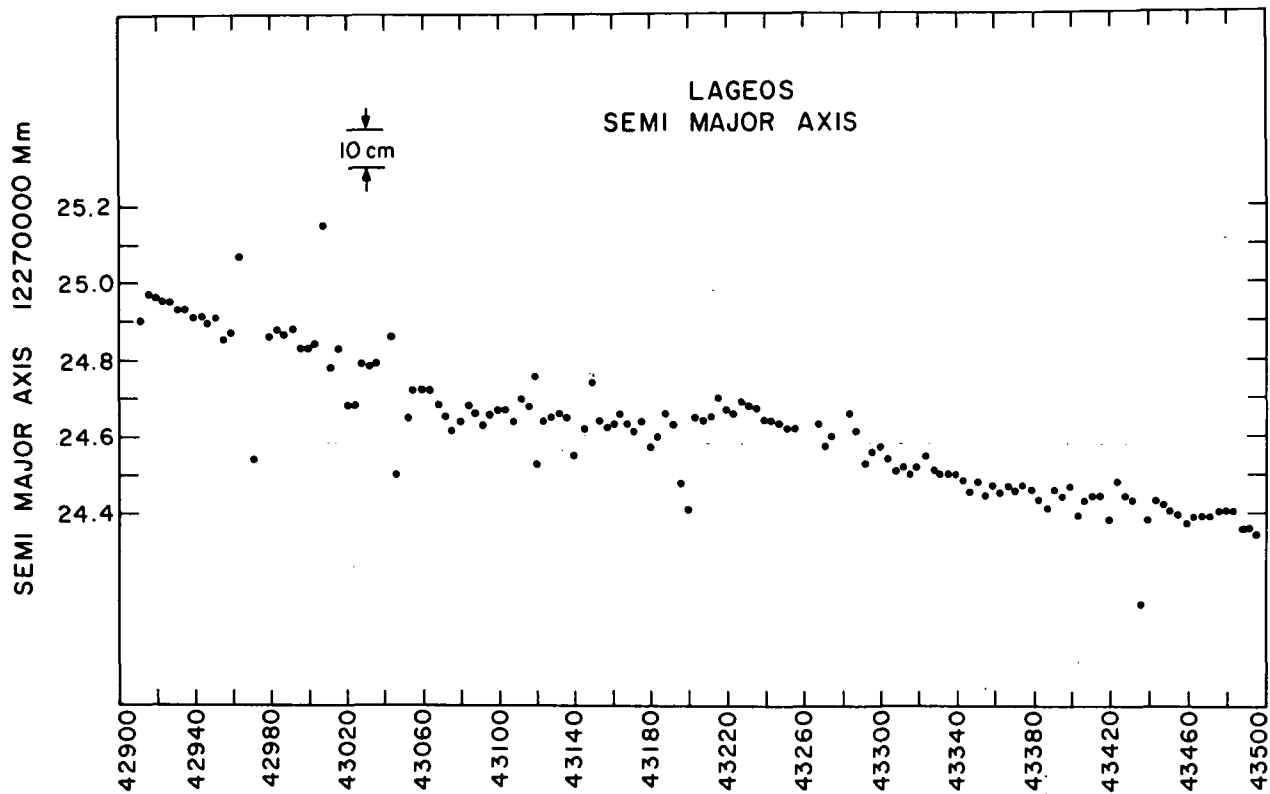


Fig. 1. Semimajor axis of Lageos.

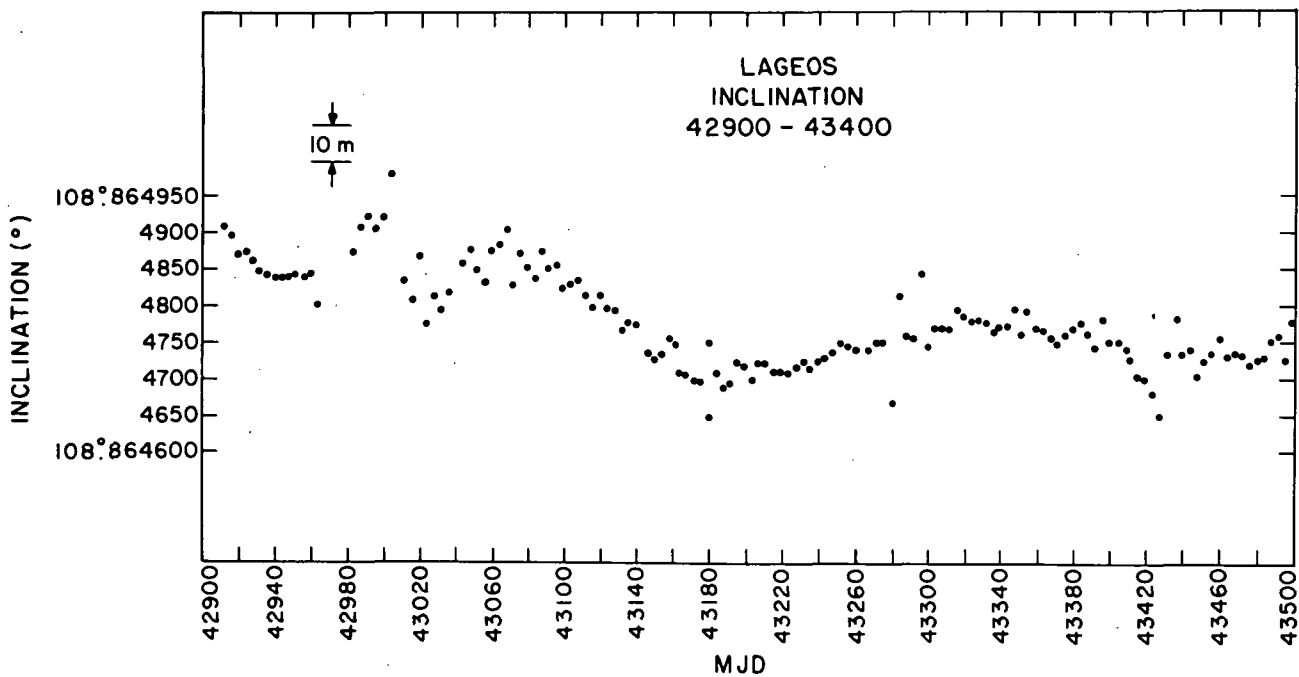


Fig. 2. Inclination of Lageos.

models, some coming from this work, the inclination and other orbital elements will be computed with greater accuracy. However, even now, some useful information can be derived on the tides; this is discussed in the following.

The study of tides is one of the fruitful applications of long-period perturbations. As

Lambeck et al. [1974] showed, ocean tides as well as body tides give rise to sensible perturbations in close-earth satellites. Currently, not enough information exists about the tides to make a definitive analysis, and preliminary results are given here to illustrate some of the difficulties. Though sensible, the perturbations are small and

TABLE 4. Data Analyzed

|                | Geos 1      | Geos 2      |
|----------------|-------------|-------------|
| Inclination    | 59°383      | 105°804     |
| $\dot{\omega}$ | 0°652/day   | -1°620/day  |
| $\dot{\Omega}$ | -2°246/day  | 1°400/day   |
| First time     | 41501 (MJD) | 41501 (MJD) |
| Last time      | 42239 (MJD) | 42278 (MJD) |
| Interval       | 738 days    | 777 days    |

a long time series is needed even to hope to get good numerical values. Other physical effects, at or near the tidal perturbation frequencies, also come into play. For example, some effects basically cannot be separated; also, there are some very fundamental gaps in our understanding.

Two series of orbits have been computed on the Geos 1 and Geos 2 satellites, as summarized in Table 4. In analyzing the mean elements, a gravity field and a Love number  $k_2$  are adopted, among other constants. We took  $k_2 = 0.29$ . The inclination of these series has been analyzed and interpreted as a perturbation due to ocean tides.

Individual tidal constituents can be isolated by the frequency. In performing harmonic analysis, we should also determine terms that should exist owing to other effects. For example, odd zonal harmonics of the gravity field will not be known without error, and hence a term in  $\sin \omega$  will arise in the data. Such a term could obviously be used to improve knowledge of the odd zonal harmonics. Also, we suspect that any analytical theory will have an error term that is called mixed secular, i.e.,  $t \cos \omega t$ , and such a term should be introduced.

The harmonic analysis was performed for the tidal constituents K2S + K2M, S2, K1S + K1M, and P1. The M2 and O1 tides could also be studied, but their periods are much shorter, 10 to 15 days. Table 5 gives the results of applying equation (1) to the observed variations in inclination. Also listed in Table 5 are the periods of the

satellite perturbations, values for some constituents from terrestrial observations [Lambeck, 1975]; and results of similar analysis by Felsentreger et al. [1976]. The fully normalized coefficients in complex form are given, together with the equivalent amplitude and phase, as is conventionally published for ease of comparison. In general, the complex tidal component is determined to about 1%.

The first thing to note is that for Geos 2, the rates of perigee  $\dot{\omega}$  and node  $\dot{\Omega}$  are almost equal and opposite. Therefore, with a relatively short time series, the terms in  $\sin/\cos \Omega$  arising from K1S + K1M cannot easily be separated from the  $\sin \omega$  term arising from the uncertainty in the odd zonal harmonic. The first values in Table 5 for that constituent represent an attempt to obtain both quantities. The second line corresponds to not including a  $\sin \omega$  term in the harmonic analysis; this result is more plausible and agrees with Felsentreger et al.

A similar circumstance occurs with K2S + K2M, in which case, we adopt values not including a  $\cos 2\omega$  term, which is equivalent to assuming no error in the even zonal harmonics.

The next point concerns the adopted value for the body tide, expressed in terms of the Love number  $k_2$ . Table 6 provides the change in the ocean tide's complex amplitude (real part only) corresponding to the change in Love number  $k_2$  from 0.29 (as adopted) to 0.302, the value obtained from Farrell [1972]. These changes are comparable to the derived amplitudes and would have a significant effect on any interpretation made of the ocean-tide values. Furthermore, if we adopt Molodensky's theoretical model for the change of Love number  $k_2$  with frequency, then the amplitudes of the derived ocean tide would be modified by the values given in the last column of Table 6.

Another aspect of the ocean tide is that each tidal constituent  $\sigma_s$  gives rise to a complete spherical-harmonics description of the ocean tide and a set of harmonics  $\mathcal{C}_{\ell m}$ . The satellite orbit

TABLE 5. Ocean Tides Determined from Satellite Data

| Tide      |         | Geos 1        |                             |                     |                             |               |                             | Geos 2              |                             |               |                             |                     |                             | Lageos        |                             |                     |                             |  |  |
|-----------|---------|---------------|-----------------------------|---------------------|-----------------------------|---------------|-----------------------------|---------------------|-----------------------------|---------------|-----------------------------|---------------------|-----------------------------|---------------|-----------------------------|---------------------|-----------------------------|--|--|
| Darwin    | Doodson | Period (days) | $\mathcal{C}_{\ell m}$ (cm) | $C_{\ell m}^+$ (cm) | $\epsilon_{\ell m}^+$ (deg) | Period (days) | $\mathcal{C}_{\ell m}$ (cm) | $C_{\ell m}^+$ (cm) | $\epsilon_{\ell m}^+$ (deg) | Period (days) | $\mathcal{C}_{\ell m}$ (cm) | $C_{\ell m}^+$ (cm) | $\epsilon_{\ell m}^+$ (deg) | Period (days) | $\mathcal{C}_{\ell m}$ (cm) | $C_{\ell m}^+$ (cm) | $\epsilon_{\ell m}^+$ (deg) |  |  |
| K2S + K2M | 275555  | 80            | 1.711 + 0.931i              | 1.26                | 29                          | 128           | 0.791 - 2.235i              | 1.53                | 289                         |               |                             |                     |                             |               |                             |                     |                             |  |  |
| S2        | 273555  | 56            | 2.660 - 0.226i              | 1.72                | 355                         | 433           | 0.598 + 0.536i              | 0.52                | 42                          |               |                             |                     |                             |               |                             |                     |                             |  |  |
| K1S + K1M | 165555  | 160           | 2.130 + 3.676i              | 5.49                | 60                          | 257           | 2.817 + 2.606i              | 2.48                | 319                         | 280           | -0.321 + 2.588i             | 1.683               | 97                          |               |                             |                     |                             |  |  |
| P1        | 163555  | 85            | -4.779 + 1.376i             | 6.42                | 164                         | 631           | 13.260 - 7.389i             |                     |                             |               |                             |                     |                             |               |                             |                     |                             |  |  |
|           |         |               |                             |                     |                             |               | 5.30 - 2.44i                | 7.54                | 335                         |               |                             |                     |                             |               |                             |                     |                             |  |  |
|           |         |               |                             |                     |                             |               | 1.707 + 1.128i              | 2.63                | 33                          | 221           | -0.349 + 2.644i             | 3.43                | 98                          |               |                             |                     |                             |  |  |

|           |        | Felsentreger et al. [1976] |                             |                     |                             |                     |                             |                     |                             |  |
|-----------|--------|----------------------------|-----------------------------|---------------------|-----------------------------|---------------------|-----------------------------|---------------------|-----------------------------|--|
|           |        | Lambeck [1975]             |                             |                     | Geos 1                      |                     |                             | Geos 2              |                             |  |
|           |        | $C_{\ell m}^+$ (cm)        | $\epsilon_{\ell m}^+$ (deg) | $C_{\ell m}^+$ (cm) | $\epsilon_{\ell m}^+$ (deg) | $C_{\ell m}^+$ (cm) | $\epsilon_{\ell m}^+$ (deg) | $C_{\ell m}^+$ (cm) | $\epsilon_{\ell m}^+$ (deg) |  |
| S2        | 273555 | 3.59*                      | 327                         | 1.7                 | 350                         | 1.0                 | 62                          |                     |                             |  |
| K1S + K1M | 165555 | 3.3                        | 318                         | 8.8                 | 345                         | 5.7                 | 334                         |                     |                             |  |
| P1        | 163555 | 0.7                        | 140                         | 5.0                 | 178                         | 4.9                 | 127                         |                     |                             |  |

\* Includes atmospheric tide.



TABLE 6. Equivalent Ocean Tide

| Tide | $D_{\ell m}$ | $\Delta C_{\ell m}$ (cm) | $k_2$  | $\Delta C_{\ell m}$ (cm) |
|------|--------------|--------------------------|--------|--------------------------|
| M2   | 0.90809      | 1.908                    | 0.3015 | 1.8288                   |
| K2   | 0.11498      | 0.242                    | 0.3015 | 0.2316                   |
| S2   | 0.42248      | .888                     | 0.3015 | 0.8508                   |
| N1   | -.53011      | -1.114                   | .2609  | 2.7014                   |
| P1   | .17543       | .369                     | .2898  | -0.0061                  |
| O1   | .37694       | .792                     | .3001  | 0.6667                   |

$$\Delta k_{\ell} = 0.302 - 0.29 = 0.012$$

responds to a linear combination of these  $\mathcal{C}_{\ell m}$ 's, where here we have determined the combined effect, i.e., a lumped coefficient. To illustrate this, consider K2S + K2M. From Geos 1, we have the value  $\mathcal{C}_{22} = 1.711 + 0.931i$  and from Geos 2,  $\mathcal{C}_{22} = 0.598 + 0.536i$ . If we assume that the only other tidal term is  $\mathcal{C}_{42}$ , we can obtain the two linear equations in two unknowns. It turns out that the factor multiplying  $\mathcal{C}_{42}$  for Geos 1 is negligible, so we immediately have

$$\overline{\mathcal{C}}_{22} = 1.711 + 0.931i$$

$$\overline{\mathcal{C}}_{42} = 7.44 + 2.64i$$

or in terms of conventional harmonics,

$$C_{22}^+ = 1.26 \text{ cm}, \quad \epsilon_{22}^+ = 28^{\circ}56'$$

$$C_{42}^+ = 1.76 \text{ cm}, \quad \epsilon_{42}^+ = 19^{\circ}5'$$

These values of  $C_{22}^+$  would have to be modified if  $k_2$  takes a value different from 0.29. However,  $C_{42}^+$  is unchanged.

#### Conclusions

The accuracy of analytical perturbation theory for short-period perturbations seems certain only to about 20 cm. It may be better than that, and additional, rather straight-forward analysis should clarify the situation. In any case, the numerical verification of analytical theory is not so simple, and the unification of a number of different developments based on different principals still requires some study.

The long-term analysis of mean elements is providing some new information about the ocean and body tides, although many questions remain to be resolved. The relation between ocean and body tides and the possible frequency dependence of  $k_{\ell}$  and the loaded Love number  $k_{\ell}^*$  must be resolved before definitive information on ocean tides can be obtained. A number of simple tests can be made, on which the currently derived values fail. They should agree with a numerical model, and the relative amplitudes of tides close in frequency should correspond to the relative amplitude of the driving force as represented by  $D_{\ell m}$ 's.

Finally, some new information should come from analysis of Lageos data. The unexplained secular decrease in semimajor axis will not hinder the planned purposes of Lageos. In all other respects, the satellite is being used as it was intended.

Acknowledgment. This work was supported in part by Contract F19628-78-C-0216 from the U.S. Air Force.

#### References

- Aksnes, K., Short-period and long-period perturbations of a spherical satellite due to direct solar radiation, *Celest. Mech.*, **13**, 89-104, 1976.
- Balmino, G., Numerical methods of orbital dynamics, in *Satellite Dynamics*, ed. by G. E. O. Giacaglia, Springer Verlag, Berlin, pp. 50-97, 1975.
- Brouwer, D., Solution of the problem of artificial satellite theory without drag, *Astron. J.*, **64**, 378-397, 1959.
- Cartwright, D. E., and A. C. Edden, Corrected table of tidal harmonics, *Geophys. J.*, **33**, 253-264, 1973.
- Deprit, A., and R. Zahar, Numerical integration of an orbit and its concomitant variations by recurrent power series, *Zeit. Angew. Math. Phys.*, **17**, 426-430, 1966.
- Doodson, A. T., The harmonic development of the tide-generating potential, *Proc. Roy. Soc. A*, **100**, 305-329, 1921.
- Farrell, W. E., Deformation of the earth by surface loads, *Rev. Geophys. Space Phys.*, **10**, 761-797, 1972.
- Felsentreger, T. L., J. G. Marsh, and R. W. Agreen, Analysis of the solid earth and ocean tidal perturbation on the orbits of the Geos-1 and Geos-2 satellites, *J. Geophys. Res.*, **81**, 2557-2562, 1976.
- Gaposchkin, E. M., Satellite orbit analysis at Smithsonian Astrophysical Observatory, in *Space Research VIII*, ed. by A. P. Mitra, L. G. Jacchia, and W. S. Newman, North-Holland Publ. Co., Amsterdam, pp. 76-80, 1968.
- Gaposchkin, E. M., Satellite dynamics, in *1973 Smithsonian Standard Earth (III)*, ed. by E. M. Gaposchkin, Smithsonian Astrophys. Obs. Spec. Rep. No. 353, pp. 85-192, 1973.
- Garfinkel, B., The orbit of a satellite of an oblate planet, *Astron. J.*, **64**, 353-367, 1959.
- Goad, C. C., and B. C. Douglas, Lunar tidal acceleration obtained from satellite derived ocean tide parameters, *J. Geophys. Res.*, **83**, 2306-2310, 1978.
- Hori, G., Theory of general perturbations with unspecified canonical variables, *Publ. Astron. Soc. Japan*, **18**, 286-296, 1966.
- Hori, G., Theory of general perturbation, in *Recent Advances in Dynamical Astronomy*, ed. by B. D. Tapley and V. Szebehely, D. Reidel Publ. Co., Dordrecht-Holland, pp. 231-249, 1973.
- Jeffreys, H., and R. O. Vicente, The theory of nutation and the variation of latitude, *Mon. Not. Roy. Astron. Soc.*, **117**, 142-161, 1957a.

- Jeffreys, H., and R. O. Vicente, The theory of nutation and the variation of latitude. The Roche model core. Mon. Not. Roy. Astron. Soc., 117, 162-173, 1957b.
- Kaula, W. M., Theory of Satellite Geodesy, Blaisdell Publ. Co., Waltham, Mass., 124 pp., 1966.
- Kinoshita, H., Third-order solution of an artificial satellite theory, Smithsonian Astrophys. Obs. Spec. Rep. No. 379, 104 pp., 1977.
- Kozai, Y., The motion of a close earth satellite, Astron. J., 64, 367-377, 1959.
- Kozai, Y., Effects of solar radiation pressure on the motion of an artificial satellite, Smithsonian Astrophys. Obs. Spec. Rep. No. 56, pp. 25-33, 1961.
- Kozai, Y., A new method to compute lunisolar perturbations in satellite motions, Smithsonian Astrophys. Obs. Spec. Rep. No. 349, 27 pp., 1973.
- Kozai, Y., and H. Kinoshita, Effects of motion of the equatorial plane on the orbital elements of an earth satellite, Celest. Mech., 7, 356-366, 1973.
- Krogh, F. T., On testing a subroutine for the numerical integration of ordinary differential equations, J. Assoc. Comp. Mach., 20, pp. 545-562, 1973.
- Lambeck, K., A. Cazenave, and G. Balmino, Solid earth and ocean tides estimated from satellite orbit analyses, Rev. Geophys. Space Phys., 12, 421-434, 1974.
- Lambeck, K., Effects of tidal dissipation in the oceans on the moon's orbit and the earth's rotation, J. Geophys. Res., 80, 2917-2925, 1975.
- Lautman, D. A., Perturbations of a close-earth satellite due to sunlight diffusely reflected from the earth, Celest. Mech., 15, 387-420, 1977a.
- Lautman, D. A., Perturbations of a close-earth satellite due to sunlight reflected from the earth. II. Variable albedo, Celest. Mech., 16, 3-25, 1977b.
- Longman, I. M., A Green's function for determining the deformation of the earth under surface mass loads. 1. Theory, J. Geophys. Res., 67, 845-850, 1962.
- Longman, I. M., A Green's function for determining the deformation of the earth under surface mass loads. 2. Computations and numerical results, J. Geophys. Res., 68, 485-496, 1963.
- Molodensky, M. S., The theory of nutation and diurnal earth tides, in Quatrième Symposium International sur les Marées Terrestres, Comm. Obs. Roy. de Belgique No. 188, Ser. Geophys. No. 58, pp. 25-56, 1961.
- Munk, W. H., and G. J. F. MacDonald, The Rotation of the Earth: A Geophysical Discussion, Cambridge Univ. Press, Cambridge, 323 pp., 1960.
- Sehna, L., and S. B. Mills, The short-period drag perturbations of the orbits of artificial satellites, Smithsonian Astrophys. Obs. Spec. Rep. No. 223, 30 pp., 1966.
- Rabe, E., Determination and survey of periodic Trojan orbits in the restricted problem of three bodies, Astron. J., 66, 500-513, 1961.
- Robertson, H. P., Dynamical effects of radiation in the solar system, Mon. Not. Roy. Astron. Soc., 97, 423-438, 1937.
- United States Naval Observatory, Improved Lunar Ephemeris, 1952-1959, Nautical Almanac Office, 422 pp., 1954.
- Velez, C. E., Stabilization and real world satellite problem, in Satellite Dynamics, ed. by G. E. O. Giacaglia, Springer Verlag, Berlin, pp. 136-153, 1975.